J Mol Model (2013) 19:5569–5577
DOI 10.1007/s00894-013-2037-z

ORIGINAL PAPER

Structures, spectroscopic and thermodynamic properties of U_2O_n (n = 0 ~ 2, 4) molecules: a density functional theory study

Peng Li · Wen-Xia Niu · Tao Gao · Fan Wang · Ting-Ting Jia · Da-Qiao Meng · Gan Li

Received: 16 January 2013 / Accepted: 11 October 2013 / Published online: 21 November 2013

Abstract The equilibrium structures, spectroscopic and thermodynamic parameters [entropy (S), internal energy (E), heat capacity (C_p)] of U_2, U_2O, U_2O_2 and U_2O_4 uranium oxide molecules were investigated systematically using density functional theory (DFT). Our computations indicated that the ground electronic state of U_2 is the septet state and the equilibrium bond length is 2.194 Å; the ground electronic state of U_2O and U_2O_2 were found to be $\widetilde{X}^3\Phi$ and $\widetilde{X}^3\sum_g$ with stable $C_{\infty v}$ and $D_{\infty h}$ linear structures, respectively. The bridge-bonded structure with D_{2h} symmetry and $\widetilde{X}^3B_{1g}$ state is the most stable configuration for the U_2O_4 molecule. Mulliken population analyses show that U atoms always lose electrons to become the donor and O atoms always obtain electrons as the acceptor. Molecular orbital analyses demonstrated that the frontier orbitals of the title molecules were contributed mostly by 5f atomic orbitals of U atoms. Vibrational frequencies analyses indicate that the maximum absorption peaks stem from the stretching mode of U–O bonds in U_2O, U_2O_2 and U_2O_4. In addition, thermodynamic data of U_2O_n (n = 0 ~ 4) molecules at elevated temperatures of 293.0 K to 393.0 K was predicted.

Keywords Uranium oxide molecule · Geometrical structure · Thermodynamic parameters · DFT calculations

P. Li · T. Gao (✉) · T.-T. Jia
Institute of Atomic and Molecular Physics, Sichuan University, Chengdu 610065, People's Republic of China
e-mail: gaotao@scu.edu.cn

W.-X. Niu
College of Physical Science and Technology, Sichuan University, Chengdu 610065, China

F. Wang (✉)
College of Chemistry of Sichuan University, Chengdu 610065, People's Republic of China
e-mail: wangf@scu.edu.cn

D.-Q. Meng · G. Li
National Key Laboratory for Surface Physics and Chemistry, Mianyang 621907, People's Republic of China

Introduction

The physical and chemical properties of the actinide elements, particularly those of uranium and plutonium, are quite important in surface and corrosion science for rational handling of nuclear materials [1, 2], and thus their oxides have received considerable attention over many years [3–10]. U_2 has been detected in the gas phase [11]. In the course of multipurpose mass spectrometric studies on high temperature vaporization of (Eu_2O_3+UO_2+WO_3) and ($EuPO_4$+UO_2) powder, $U_2O_{4\ (g)}$ species were identified, for the first time, as minor components of the vapors by Guido et al. [12], who discussed a tentative quantity for the already known $U_2O_{2\ (g)}$.

The experimental techniques discussed above unquestionably provide novel information on uranium oxides. However, limitations remain in terms of detailed information such as the structures, spectroscopic and thermodynamic properties of these oxides. Quantum chemistry calculations are now reaching a level of sophistication where they may provide results for lanthanide and actinide compounds with reasonable accuracy. These advantages offer the possibility that actinide chemistry may soon be explored by computational methods, thereby avoiding many hazardous and expensive experimental studies [4]. Nevertheless, the study of uranium molecules still presents a challenge for both experimental and theoretical researchers. The nearly degenerate 5f, 6d, 7s, and 7p orbitals give rise to a multitude of possible configurations with large numbers of electrons, open f and d shells, and strong relativistic effects must be taken into account [7, 10]. The molecular

structures of $UO_{n(g)}$ (n=1–3) have been studied in detail through theoretical and experimental study [5–9], but more complicated binding may occur when the oxides have more than one U atom, and such behavior is common with nuclear oxides. Studies exploring the stability of unusual uranium oxide molecule structures in addition to the known $UO_{n(g)}$ (n=1–3) may be of importance in pressure-volume-temperature data measurement at elevated temperatures. Therefore, we extended our research to the case of U_2O_n (n=0–2, 4) molecules. For the U_2 molecule, Pepper et al. [13] used the complete active space self–consistent field (CAS-SCF) method and single-reference CI (SRCI) calculations to describe the bonding in this system; they found that U_2 had a $^5\Sigma^+_g$ ground state and an equilibrium bond distance of 2.20 Å. Wang et al. [14] carried out a systemic DFT study for U_2. The nonet ground state ($^9\Sigma_g$), long bond length of 3.89 Å and short bond length of 2.99 Å for the U_2 dimer were obtained from the latter report. Gagliardi et al. [15, 16] employed the CAS-SCF method to study bond length, electronic structure and chemical bonding of the U_2 molecule. Their calculations showed that the U_2 molecule has a quintuple bond and the ground state is a septet state, corresponding to an equilibrium bond distance of 2.43 Å.

However, to our knowledge, experimental data on the molecular structure of U_2O_n (n=1–2, 4) are scarce, and there are also no theoretical studies on the geometric or electronic structure of U_2O_n (n=1–2, 4). The main goal of present work was to perform a detailed theoretical study of U_2O, U_2O_2 and U_2O_4 molecules. We focused our attention on four aspects: (1) to explore the ground state structure of U_2O, U_2O_2 and U_2O_4 molecules; (2) to analyze the population properties and bond order of U_2, U_2O, U_2O_2 and U_2O_4 molecules; (3) to gain infrared spectral data for U_2O, U_2O_2 and U_2O_4; and (4) to calculate the thermodynamic parameters (S, E, C_p) of U_2O_n (n=0–4) gases. A "Computational methods" section is followed by "Results and discussion", including geometries and electronic properties, population properties, bond orders, spectrum analysis, and thermodynamic parameters. Some final remarks are summarized in the "Conclusions" section.

Computational methods

The geometries, vibrational frequencies and thermodynamic data of the title molecules were calculated using relativistic density function theory (DFT) as implemented in ADF 2009.01 [17–26]. Lyon et al. [27] used ADF to study the formation of unprecedented actinide≡carbon triple bonds. Zhang et al. [28] investigated the molecular structures and vibrational frequencies for uranium hexahalides UX_6 (X=F, Cl, Br and I) with the same software. Their results were in good agreement with recent experimental data. Previously, DFT has been applied with great success to determining the physical and chemical properties of uranium and plutonium compounds [27, 29, 30]. We employed spin-polarized generalized gradient approximation (GGA) with OPTX [31] exchange with PBE correlation (OPBE) [32] functional for the exchange and correlation (XC) interaction, and TZP basis sets (contains valence triple zeta and one polarization function) [33]. The scalar relativistic (SR) zero order regular approximation (ZORA) [19, 34] was adopted to account for significant relativistic effects. SCF calculations were performed with a convergence criterion of 10^{-6} Hartree on the total energy. We carried out geometrical optimization with the convergence criterion as follows: 10^{-5} Hartree for the total energy, 10^{-5} Hartree/Å for the gradient and 10^{-3} Å for the bond length. Spin–unrestricted calculations were then performed for all possible spin multiplicities. Due to the importance of the 6s and 6p orbitals for uranium bonding, they are included explicitly in the variational space along with the 5f, 6d and 7s valence orbitals. Therefore, the [$1s^2$] core for O and [$1s^2 5d^{10}$] core for U were treated via frozen core approximation. To evaluate the accuracy of the current computational scheme (OPBE/ZORA-SR), test calculations were performed for relative energies of atomic level splitting of the U atom. Our calculated results at the OPBE/ZORA-SR level along with available experimental values are summarized in Table 1. We can see that the approaches used in this study give results in agreement with available experimental values. In addition, we calibrated the current approach with a previous theoretical study of equilibrium geometries for uranium oxides (UO, UO_2, UO_3 and U_2O_3) [36], and found that the equilibrium geometries were well reproduced by the OPBE/ZORA-SR method. Finally, we analyzed the effect of spin–orbit interaction by performing single-point calculations on the optimized geometries obtained at the OPBE/ZORA level within the spin–orbit ZORA approximation (OPBE/SO-ZORA).

Results and discussion

Structures and frequency analysis

Dozens of possible geometries have been designed for U_2O_n (n=0~2, 4) molecules to obtain minimum energy structures. We performed geometry optimization for all possible spin multiplicity of the title molecules, and computed energies for

Table 1 Relative energies (in kcal/mol) of energy levels for U atom

Species	Our work	Experimental [a]
[Rn]$5f^3 6d 7s^2$ (3)	10.16	17.12
[Rn]$5f^3 6d 7s^2$ (5)	0.00	0.00
[Rn]$5f^3 6d^3$ (7)	52.54	66.01

[a] Statistically averaged spin orbit energy levels taken from [35]

Table 2 The multiplicity (M), point group (PG), total energies (E), electronic state (E_S) and bond length (R) for the stable structures of U_2O_n (n=0–2, 4) molecules

Mole	M	PG	E_S	E (eV)	ΔE (eV)[a]	E_{SO} (eV)[b]	ΔE_{SO} (eV)[b]	R (Å)
U_2	5	$D_{\infty h}$	$^5\Sigma_g$	−9.936	0.32	−14.23	0.42	R(U-U)=2.192
	7	$D_{\infty h}$	$^7\Phi_u$	−10.256	0.00	−14.65	0.00	R(U-U)=2.194/2.20 [13]/2.43 [15]
	9	$D_{\infty h}$	$^9\Delta_g$	−9.395	0.86	−12.33	2.32	R(U-U)=2.302
U_2O	3	$C_{\infty v}$	$^3\Phi$	−21.061	0.00	−25.67	0.00	R(U-U)=2.224 R(U-O)=1.813
	9	$D_{\infty h}$	$^9\Sigma_g$	−18.130	2.93	−21.17	4.50	R(U-O)=2.035
	5	C_{2v}	$^5A_1$	−20.621	0.44	−24.90	0.77	R(U-U)=2.201 R(U-O)=2.507
U_2O_2	3	$D_{\infty h}$	$^3\Sigma_g$	−32.389	0.00	−36.57	0.00	R(U-U)=2.237 R(U-O)=1.809/2.04 [12]
	5	C_{2v}	$^5A_2$	−30.741	1.65	−35.05	1.52	R(U-U)=2.280 R(U-O)=2.065
	5	C_s	$^5A'$	−25.435	6.95	−34.36	2.21	R(U-U)=2.931 R(U_1-O_1)=2.141 R(U_2-O_1)=2.144 R(U_2-O_2)=1.940
U_2O_4	3	D_{2h}	$^3B_{1g}$	−50.831	0.00	−55.24	0.00	R(U-U)=2.437 R(U-$O_{3,4}$)=2.087 R(U-$O_{1,2}$)=1.820/1.82 [12]
	3	D_{2h}	$^3A_1$	−48.220	2.61	−54.13	1.11	R(U-U)=4.173 R(U-O)=1.834
	5	D_{2d}	$^5B_1$	−49.268	1.56	−54.62	0.62	R(U-U)=2.495 R(U-O)=1.845

[a] Difference from ground state energy

[b] Frozen core TZP for Th and O atoms, ZORA-SO results

a number of points in the neighborhood of the equilibrium structure to achieve a global minimum energy structure. The results including the multiplicity (M), point group (PG), electronic state (E_S), total energies (E) and bond distance (R) of the stable structures are listed in Table 2; Fig. 1 presents the stable isomers of U_2O, U_2O_2 and U_2O_4 molecules.

As shown in Table 2, the ground state of U_2 is a septet state (six unpaired electrons with parallel spin) with an equilibrium bond length of 2.194 Å; the corresponding ground state is $X^7\Phi_u$. Our results are consistent with those of Gagliardi et al. [15], who also indicated that the most stable electronic state of U_2 was a septet state, and all spins are predicted to be parallel (ferromagnetic coupling), which can be attributed to 'exchange stabilization': if all open-shell electrons have the same spin, the interaction between the non-bonding *5f* electrons is energetically more favorable than the antiferromagnetic coupling of the *5f* electrons. On the other hand, our U_2 bond distance is shorter than their value (2.43 Å). Nevertheless, our result for the U–U bond distance is in agreement with early theoretical studies by Pepper et al. [13], where U_2 was found to have an equilibrium bond distance of 2.20 Å, although they predicted the ground electronic state was $^5\Sigma^+_g$. Furthermore, using the B3LYP method with the relativistic effective core potential and contract valence electron basis set, Wang et al. [14] predicted that the ground state of the dimer U_2 should be $X^9\Sigma_g$, with a long bond distance of 3.89 Å and short bond 2.99 Å, respectively. Predicting the ground electronic state of U_2 is a challenging task and we report here only the result obtained according to our calculations.

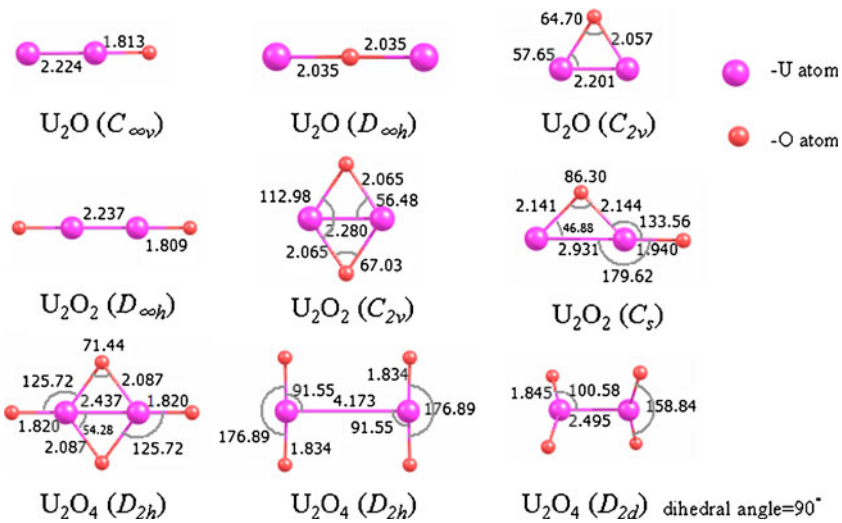

Fig. 1 Stable isomers of U_2O, U_2O_2 and U_2O_4 molecules

Table 3 Population properties for U_2, U_2O, U_2O_2 and U_2O_4 molecules

Molecule	Atom	Net charge	Spin density	Total
U_2	U_1	0.0000	3.0000	[core] $5f^{3.212}$ $6p^{5.907}$ $6d^{1.858}$ $(6s+7s)^{3.023}$
	U_2	0.0000	3.0000	[core] $5f^{3.212}$ $6p^{5.907}$ $6d^{1.858}$ $(6s+7s)^{3.023}$
U_2O	U_1	−0.0676	1.1206	[core] $5f^{3.282}$ $6p^{6.116}$ $6d^{1.436}$ $(6s+7s)^{3.234}$
	U_2	0.7464	0.8955	[core] $5f^{3.195}$ $6p^{5.851}$ $6d^{1.579}$ $(6s+7s)^{2.628}$
	O_1	−0.6788	−0.0162	[core] $2s^{1.996}$ $2p^{4.651}$
U_2O_2	U_1	0.6656	1.0241	[core] $5f^{3.183}$ $6p^{5.864}$ $6d^{1.605}$ $(6s+7s)^{2.683}$
	U_2	0.6656	1.0241	[core] $5f^{3.183}$ $6p^{5.864}$ $6d^{1.605}$ $(6s+7s)^{2.683}$
	O_1	−0.6656	−0.0241	[core] $2s^{1.999}$ $2p^{4.634}$
	O_2	−0.6656	−0.0241	[core] $2s^{1.999}$ $2p^{4.634}$
U_2O_4	U_1	1.4908	1.1076	[core] $5f^{2.999}$ $6p^{5.722}$ $6d^{1.449}$ $(6s+7s)^{2.339}$
	U_2	1.4908	1.1076	[core] $5f^{2.999}$ $6p^{5.722}$ $6d^{1.449}$ $(6s+7s)^{2.339}$
	O_1	−0.6882	−0.0545	[core] $2s^{2.006}$ $2p^{4.647}$
	O_2	−0.6882	−0.0545	[core] $2s^{2.006}$ $2p^{4.647}$
	O_3	−0.8026	−0.0531	[core] $2s^{1.995}$ $2p^{4.767}$
	O_4	−0.8026	−0.0531	[core] $2s^{1.995}$ $2p^{4.767}$

The U_2O molecule forms a stable linear equilibrium structure with U–O and U–U bond distances of 1.813 Å and 2.224 Å, respectively, as can be seen from Fig. 1. The ground electronic state of U_2O molecule is identified as the $\widetilde{X}^3\Phi$ state. On the other hand, the ground electronic state of U_2O_2 is found to be the $\widetilde{X}^3\sum_g$ state with $D_{\infty h}$ symmetry and U–O and U–U bond distances of 1.809 Å and 2.237 Å, respectively. The bridge-bonded structure with D_{2h} symmetry and $\widetilde{X}^3B_{1g}$ state is found to be the most stable configuration for the U_2O_4 molecule. As can be seen from Fig. 1, the $\widetilde{X}^3B_{1g}$ state of U_2O_4 exhibits a U–U bond distance of 2.437 Å and a pyramidal U–O–U bond angle of 71.44°. In addition, the expectation value for S^2 ($<S^2>$) is 2.015, which indicates an insignificant spin contamination.

In Table 2, we also listed the energies calculated by spin–orbit ZORA approximation. One can see that the spin–orbit ZORA method improves the relative energies of different molecular structures compared with ZORA-SR, but does not change the order of relative energy. This is consistent with the experimental results of Andrews and collaborators [3, 37], who found that, for uranium molecular systems, spin-orbit corrections have little effect on their computed geometries.

The calculated harmonic frequency of the ground state U_2 molecule is 325.75 cm^{-1}. The maximal IR intensity peak of the ground state structure of the U_2O molecule is at 870.59 cm^{-1} with an infrared intensity of 427.283 km/mol, and the vibrational mode corresponds to U–O bond stretching. Two absorption peaks can be seen in the U_2O_2 absorption spectra with the maximal IR peak at 867.11 cm^{-1}. The U_2O_4 IR spectra exhibit more absorption peaks and the maximal IR absorption intensity peak is located 867.43 cm^{-1}. All the maximal IR absorption intensity peaks of the U_2O, U_2O_2 and U_2O_4 molecule correspond to stretching of the U–O bond.

Population analysis and frontier orbitals

The charge population properties and spin density of the ground state for U_2, U_2O, U_2O_2 and U_2O_4 molecules are presented to further illustrate the electronic structure. The results are detailed in Table 3, and the symbols (U_1, O_2 etc.) in the table are in accordance with those in Fig. 2.

As can be seen from Table 3, the two uranium atoms in U_2 are neutrally charged, as expected. For the U_2O molecule, the uranium atom, which was in the middle of the molecule (as shown in Fig. 2), is negatively charged to some extent, which may be an artificial result of Mulliken population analysis. For other uranium oxides, the uranium atom always loses an electron and acts as the electron donor, while the oxygen atom always obtains electron as the electron acceptor.

The charge population results indicate that the 5f, 6d and 7s orbitals of the uranium mix with the 2p orbital of oxygen in U_2O, U_2O_2 and U_2O_4 molecules. As shown by the charge population results listed in Table 3, the number of electrons in

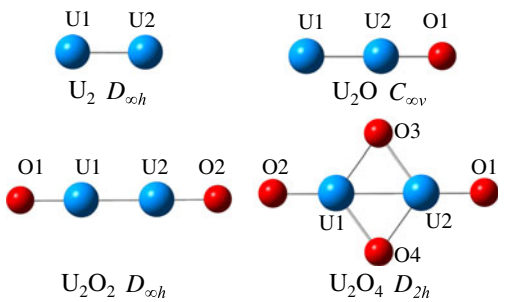

Fig. 2 Ground state structures of U_2, U_2O, U_2O_2 and U_2O_4 molecules

Table 4 HOMO and LUMO percentages (%) for ground state of U_2O_4 molecule (D_{2h})

U_2O_4	MO -L	Irreducible representation	Occupation	U (%)	O (%)
α	HOMO	B_{2u}	1	f:y 88.47	
				$f:z_{2y}$ 6.45	
				p:y 2.01	
	LUMO	B_{2g}	0	f:x 99.71	
β	HOMO	A_g	1	$f:z^3$ 52.01	
				$d:z^2$ 13.87	
				$d:_{x2-y2}$ 9.51	
				f:z 7.32	
				p:z 4.88	
	LUMO	B_{3u}	0	$f:z_{2x}$ 66.24	
				d:xz 20.5	
				f:x 6.08	
				p:x 5.43	

6s+7s orbitals of the uranium atom in uranium oxides is less than that in the same orbitals of a neutral uranium atom, which have four electrons. Meanwhile, the number of electrons in the 2p orbital of the oxygen atom is larger than that in an isolated oxygen atom, which has four electrons. Charge transfers from the 7s orbital of uranium to the 5f, 6d orbitals of uranium and 2p orbitals of oxygen. These significant hybridizations or orbital mixing between 5f, 6d and 7s orbitals of uranium and the 2p orbital of oxygen will enhance the bonding strengths of the U–O bonds. This property is consistent with our recent study [36] on UO_3 and U_2O_3 molecules.

The net charge distributions of the two oxygen atom in U_2O_2 are close to those of the corresponding oxygen atoms in U_2O_4 (O1 and O2). As can be seen from Table 3, the U_2O_2 exhibits net charges of $U_{1,2}$ (0.6656) and $O_{1,2}$ (−0.6656). The charge of the two chemically bonded oxygen atoms is about −1.32 for U_2O_2, and the same charge is depleted from the two U atoms in U_2O_2. On the other hand, net charges in U_2O_4 are $U_{1,2}$ (1.4908), $O_{1,2}$ (−0.6882) and $O_{3,4}$ (−0.8026).

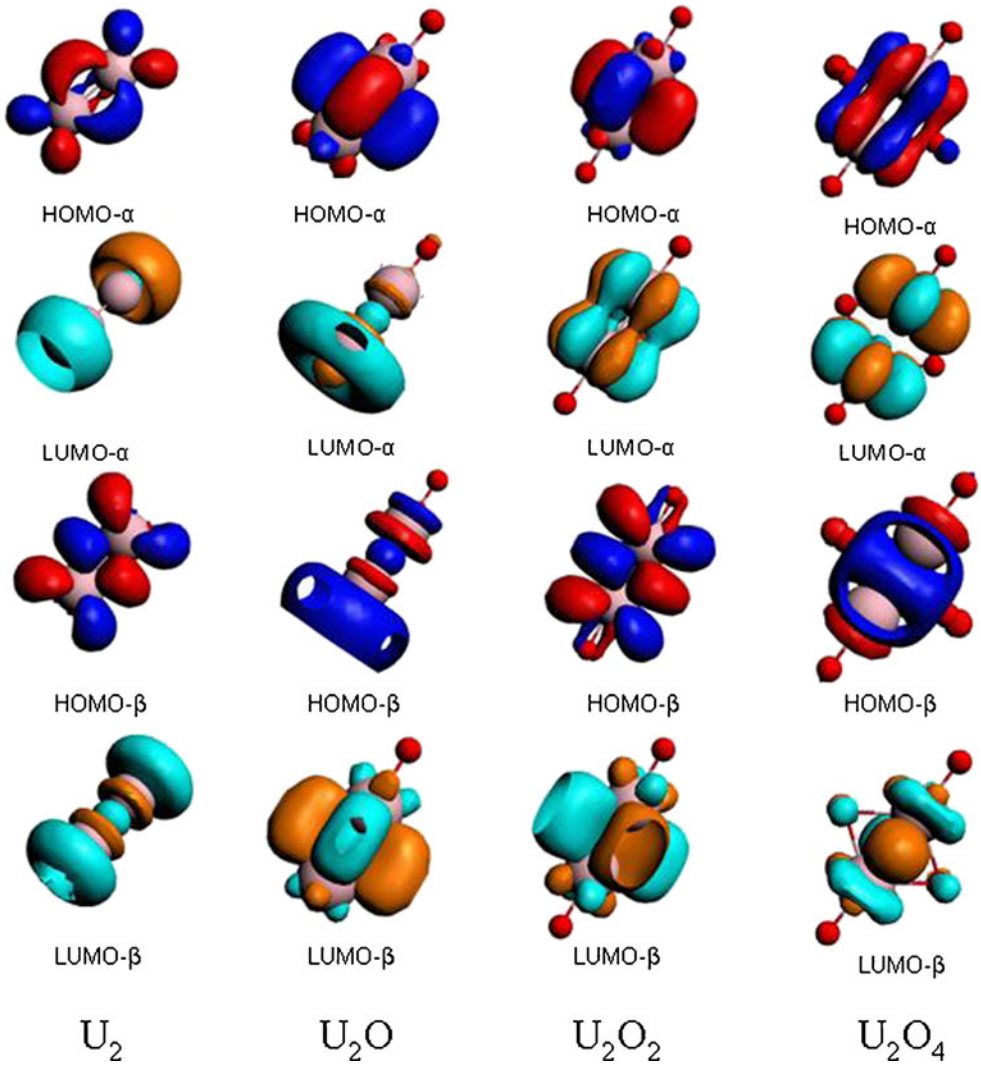

Fig. 3 Frontier molecular orbitals of ground-state structures of U_2, U_2O, U_2O_2 and U_2O_4 molecules

Table 5 Bond orders analysis for the U_2, U_2O, U_2O_2 and U_2O_4 molecules

Molecule	Species	BO_{GJ} [a]	BO_{NM} [b]
U_2	U_1-U_2	5.92	6.67
U_2O	U_1-O_1	2.39	2.90
	U_1-U_2	5.04	6.54
U_2O_2	U_1-O_1	2.41	2.95
	U_2-O_2	2.41	2.95
	U_1-U_2	4.87	5.88
U_2O_3[c]	U_1-O_1	1.14	1.44
	U_1-O_2	1.14	1.44
	U_1-O_3	1.14	1.44
	U_2-O_1	1.14	1.44
	U_2-O_2	1.14	1.44
	U_2-O_3	1.14	1.44
	U_1-U_2	3.12	3.52
U_2O_4	U_1-O_2	1.16	1.42
	U_1-O_3	1.16	1.42
	U_1-O_4	2.33	2.78
	U_2-O_1	1.16	1.42
	U_2-O_3	2.33	2.78
	U_2-O_4	1.16	1.42
	U_1-U_2	2.77	3.15

[a] BO_{GJ}, Gophinatan-Jug bond order

[b] BO_{NM}, Nalewajski-Mrozek bond order

[c] From our recent study [36]

Consequently, the two U atoms are depleted by about 3.0e in total due to the presence of four oxygen atoms in U_2O_4. Therefore, more charge is depleted from U atoms in U_2O_4 than those in U_2O_2. Based on this result, we predict that an additional O atom approaching U_2O_4 might assist in further oxidizing of U_2O_4, and result in forming stable higher oxides.

The spin densities of the unpaired electrons are distributed among the U and oxygen atoms. The uranium atom makes a positive contribution to the total spin multiplicity in U_2O, U_2O_2 and U_2O_4 molecules, while oxygen always contributes a negative spin. For U_2 molecule, the overall six valence electron spins are parallel and the two uranium atoms have the same spin density. The ground state of U_2O_4 exhibits a distribution of spin densities as U (1.1076), $O_{1,\ 2}$ (−0.0545), and $O_{3,\ 4}$ (−0.0531). This suggests a more significant spin localization on U in the case of the U_2O_4 molecule; therefore, the unpaired electron concentrates mainly on the U atom.

Molecular orbital analyses show that the frontier orbitals of U_2, U_2O, U_2O_2 and U_2O_4 molecules were contributed mostly by 5f orbitals of U atoms. Taking U_2O_4 molecule as an example, the contributions to HOMO and LUMO of the ground state U_2O_4 molecule in terms of atomic orbitals are listed in Table 4. The electrophilic attack would occur preferentially at the HOMO site [38], and we can thus predict that an additional O atom attacking the U_2O_4 molecule (bridge-bonded structure with D_{2h} symmetry) may form a bond with the U atoms in U_2O_4 preferentially. The frontier molecular orbitals of ground-state structures of U_2, U_2O, U_2O_2 and U_2O_4 molecules are presented in Fig. 3. As shown by the frontier molecular orbitals, HOMO is the bonding orbital between the two U atoms. The two HOMOs of U_2 are π-type bonds, which correspond to the $6d\pi_u$ orbitals in Gagliardi's work [15].

Bond order gives an indication of the stability of a bond and is also an index of bond strength. The bond orders analyses [39, 40] of small molecules are listed in Table 5. The symbols (U_1, O_2 etc.) in the table are consistent with those in Fig. 2. As shown in Table 5, with the U–O coordinate number increasing, the U–O bond order decreases. Our calculations also reveal that the U–U bond distances and bond orders depend on the U–O coordinate number around the U atoms. For the U_2 molecule, there are no electronegative oxygens to support a large positive charge on the U atoms; the U–U bond is the strongest (bond order is 5.92) and has the shortest U–U distance (2.194 Å). With an increasing number of oxygen atoms around the U_2 molecule, the strength of the U–U bond is gradually weakened (bond orders in U_2O, U_2O_2 and U_2O_4 are 5.04, 4.87 and 2.77, respectively), and the U–U bond length becomes longer (bond lengths of U_2O, U_2O_2 and U_2O_4 are 2.224 Å, 2.237 Å and 2.437 Å, respectively). The U–U bond in U_2O_3 is weaker than in U_2O_4 and this disaccord is due to the special structure of the U_2O_3 molecule. The ground-state structure of the U_2O_3 molecule has been identified as a trigonal bipyramid conformation [36], with three oxygen atoms in the bisecting plane of two uranium atoms, shared by the two uranium atoms. This makes the U–U bond of U_2O_3 weaker than that in U_2O_4.

Bond orders alone with force constants and dissociation energy of U–U bond in U_2O, U_2O_2 and U_2O_4 molecules are reported in Table 6. No direct correlation was found between bond order and bond dissociation energy. The OU-U/OU-UO pair is a good illustration. Similarly, this view was also confirmed by the studies of Roos and collaborators. [41] They pointed out that the bond energy is a complex quantity that depends on atomic promotion energy and the interplay between attractive nuclear forces and electron repulsion, among other factors. The force constant (k) is a measure of the strength of the

Table 6 Bond orders correlate with force constants and dissociation energy of the U–U bond in U_2O, U_2O_2 and U_2O_4 molecules

Molecule	Species	Bond orders		Force constants (N/M)	D_e (U–U) (eV)
		BO_{GJ}	BO_{NM}		
U_2O	OU-U	5.04	6.54	726.44	4.93
U_2O_2	OU-UO	4.87	5.88	759.83	5.56
U_2O_4	2OU-UO2	2.77	3.15	480.62	4.27

Table 7 The entropy (S)[a] heat capacity (C_p)[a] and internal energy (E)[b] of U_2O_n molecules

T(K)	U_2			U_2O			U_2O_2			U_2O_3			U_2O_4		
	S	E	C_p	S	E	C_p	S	E	C_p	S	E	C_p	S	E	C_p
293	63.72	10.96	8.57	73.92	27.27	13.03	82.18	43.55	17.47	82.39	55.60	21.42	93.76	69.16	23.97
298	63.86	11.13	8.58	74.14	27.53	13.06	82.48	43.89	17.53	82.75	56.02	21.54	94.17	69.62	24.08
313	64.29	11.50	8.61	74.79	28.20	13.16	83.34	44.85	17.69	83.82	57.27	21.85	95.36	71.04	24.39
353	65.33	12.63	8.68	76.38	30.08	13.39	85.49	47.53	18.09	86.49	60.66	22.55	98.34	74.85	25.12
393	66.26	13.76	8.73	77.83	32.00	13.58	87.46	50.25	18.44	88.94	64.15	23.09	101.1	123.9	25.76

[a] In Cal/mol-Kelvin

[b] Internal energy (E) including the zero-point energy, in kJ/mol

interaction of atoms. A correlation between force constant and bond dissociation energy was found—an increase in force constant as the bond dissociation energy increased.

Thermodynamic properties

Entropy (S), internal energy (E), and heat capacity (C_p) are fundamental thermodynamic parameters that provide insight into binding strength, the energies of nuclear materials and the nature of the actinide material [42]. The S, E and C_p for the lowest energy structures of U_2O_n (n=0–4) molecules at temperatures ranging from 293.0 K (about 20°C) to 393.0 K (about 120°C) are listed in Table 7. The U_2O_3 with trigonal bipyramid structure obtained in our previous study [36] was used in the thermodynamics calculation. As can be seen from Table 7, the increase in entropy with temperature could be the consequence of a more disordered U_2O_n (n=0–4) structure at elevated temperatures due to perturbation by thermal movements. The heat capacities (C_p) of these molecules also increase as the temperature increases. The internal energy of U_2O_n (n=0~4) shows the molecules become more endothermic as the temperature increases.

We computed the standard enthalpies of formation for UO, U_2O_2, U_2O_3 and U_2O_4, and compared them with available experimental data to verify the rationality of the molecular structure we determined. The standard enthalpy of the formation of molecules can be derived from the molecular dissociation energy and heat of sublimation through constructing a Hess cycle. According to Hess's law, if a reaction can be carried out in a series of steps, the sum of the enthalpies for each step equals the enthalpy change for the overall reaction. Detailed discussions on the calculation of the standard enthalpy of formation can be found in the literature [43]. The dissociation energies of UO, U_2O_2, U_2O_3 and U_2O_4 are listed in Table 8.

Taking UO (g) as an example, the standard enthalpy of formation can be determined by the following equation:

$$1/2O_2(g) + U(s) \rightarrow UO(g) \quad (1)$$

The change in enthalpy of the above equation equals the energy released in the each step reaction using the following cycle:

$$U(s) = U(g) \quad \Delta H_1 = 535.6 \text{ kJ/mol} \quad (2)$$

[44, 45]

$$1/2\,O_2(g) = O(g) \quad \Delta H_2 = 251.248 \text{ kJ/mol} \quad (3)$$

$$U(g) + O(g) = UO(g) \quad \Delta H_3 = -771.592 \text{ kJ/mol} \quad (4)$$

By summing the enthalpies for each step above, we obtain ΔH_f=15.45 kJ/mol^{-1}. Applying the same method, the standard enthalpy of formation for U_2O_2, U_2O_3 and U_2O_4 molecules were calculated and the results are listed in Table 9.

From Table 9, we first note that the standard enthalpy of formation for UO is 15.45 kJ/mol^{-1}, which is in good

Table 8 Energy (E) of U, O atoms and UO, U_2O_2, U_2O_3 and U_2O_4. Dissociation energy (D_e) of UO, U_2O_2, U_2O_3 and U_2O_4 molecules

	$E_{[UnOm]}$ (kJ/mol)	$E_{[U]}$ (kJ/mol)	$E_{[O]}$ (kJ/mol)	D_e (kJ/mol)
UO	−1,245.72	−262.25	−211.88	−771.59/−759.34 [a]
U_2O	−2,032.07	−262.25	−211.88	−1,296.90
U_2O_2	−3,125.06	−262.25	−211.88	−2,176.80
U_2O_3	−3,903.99	−262.25	−211.88	−2,743.79
U_2O_4	−4,904.44	−262.25	−211.88	−3,532.35

[a] Experimental D_e [46]

Table 9 Standard enthalpy of formation for UO, U_2O, U_2O_2, U_2O_3 and U_2O_4 molecules

	$\Delta H_f{}^o$(kJ/mol)	$\Delta H_f{}^o$ (experimental) (kJ/mol)
UO(g)	15.45	19.9±10 [47]
U_2O (g)	26.86	—
U_2O_2(g)	−602.72	−391±36 [12][a]
U_2O_3(g)	−918.22	−808±29 [12][a]
U_2O_4(g)	−1,455.29	−1,262±26 [12][a]

[a] Proposed value

agreement with experimental results. The results of U_2O_3 and U_2O_4 are 10 % and 13 % larger than experimental data, respectively, while these results are still in reasonable agreement with experimental values. On this basis, the standard enthalpy of formation for U_2O is predicted to be 26.86 kJ/mol^{-1}. Nevertheless, our result for U_2O_2 deviates from experimental values to a larger degree (50 %). Besides the error in the chosen XC functional, these deviations may also be related to uncertainty of the ground state energy of the U and O atom, which will further give rise to uncertainties on the dissociation energy of the title molecules. Most atoms have degenerate ground states; this leads to uncertainties of 13–20 kJ/mol^{-1} in the atomic ground state energy of second and third period main group elements and the first transition series [48]. This uncertainty is expected to be large for U. Overall, the reasonable agreement of the standard enthalpy of formation between theoretical and available experimental data available justify the optimized structures of U_2O_n (n =0–2, 4) molecules in another respect.

Conclusions

The stable structures of U_2, U_2O, U_2O_2 and U_2O_4 molecules were investigated systematically based on DFT calculations. Our computations indicate that the ground electronic state of the U_2 molecule was the $X^7\Phi_u$ state, with an equilibrium bond length of 2.194 Å; the ground electronic state of U_2O and U_2O_2 was found to be $\widetilde{X}^3\Phi$ and $\widetilde{X}^3\Sigma_g$ with stable $C_{\infty v}$ and $D_{\infty h}$ linear structures, respectively. The bridge-bonded structure with D_{2h} symmetry and $\widetilde{X}^3B_{1g}$ state is found to be the most stable configuration for the U_2O_4 molecule.

The charge population property, spin density and bond order of U_2, U_2O, U_2O_2 and U_2O_4 molecules have been discussed. The results demonstrate a charge transfer from uranium atom to oxygen atom, and orbital mixing between 5f, 6d and 7s orbitals of uranium and the 2p orbital of oxygen. Spin density analysis indicates that, for the U_2 molecule, the directions of spin for the overall six unpaired valence electron are parallel, and two uranium atoms have the same spin density. The uranium atom makes a positive contribution to total spin multiplicity for U_2O, U_2O_2 and U_2O_4, while oxygen always contributes to negative spin. Molecular orbital analyses showed that the frontier orbitals of U_2, U_2O, U_2O_2 and U_2O_4 molecules were comprised mostly of 5f atomic orbitals of U atoms.

The harmonic frequency of the ground state for U_2 molecule is at 325.75 cm^{-1}, and the maximal IR peaks of the ground state structure of U_2O, U_2O_2 and U_2O_4 are at 870.59 cm^{-1}, 867.11 cm^{-1} and 867.43 cm^{-1}, respectively; these maximal IR peaks correspond to the vibration of oxygen atoms.

The entropy, internal energy, and heat capacity (C_p) for the lowest energy structures of U_2O_n (n =0–4) molecules at temperatures ranging from 293.0 K to 393.0 K have been calculated. Our results show that enthalpy and heat capacity increases with higher temperature; the results of internal energy indicate that the molecules become more endothermic as the temperature increases. The standard enthalpies of formation for UO, U_2O_2, U_2O_3 and U_2O_4 were also calculated and compared with available experimental data to verify the rationality of the obtained molecular structure.

Acknowledgments We are very grateful to Dr X. F. Tian for many helpful discussions. Our thanks are also due to Y. F. Gao for practical help. We would like to thank the reviewers for their valuable suggestions on improving our paper. This research was supported by Open Fund of State Key Laboratory of Information Photonics and Optical Communications (Beijing University of Posts and Telecommunications, P.R. China).

References

1. Korzhavyl PA, Leventevitos, Andersson DA, Johansson B (2004) Nat Mater 3:225–228
2. Haschke JM, Allen TH, Morales LA (2000) Los Alamos Sci 26:252–273
3. Gagliardi L, Roos BO, Malmqvis PÅ, Dyke JM (2001) J Phys Chem A 105:10602–10606
4. Lue CJ, Jin J, Ortiz MJ, Rienstra-Kiracofe JC, Heaven MC (2004) J Am Chem Soc 126:1812–1815
5. Zhou M, Andrews L, Ismail N, Marsden C (2000) J Phys Chem A 104:5495–5502
6. Pyykkö P, Li J, Runeberg N (1994) J Phys Chem 98:4809–4813
7. Gagliardi L, Heaven MC, Krogh JW, Roos BO (2005) J Am Chem Soc 127:86–91
8. Green DW, Reedy GT, Gabelnick SD (1980) J Chem Phys 73:4207
9. Li J, Bursten BE, Andrews L, Marsden CJ (2004) J Am Chem Soc 126:3424–3425
10. Infante I, Eliav E, Vilkas MJ, Ishikawa Y, Kaldor U, Visscher L (2007) J Chem Phys 127:124308
11. Gingerich KA (1980) Symp Faraday Soc 14:109–125
12. Guido M, Balducci G (1991) J Chem Phys 95:5373
13. Pepper M, Bursten BE (1990) J Am Chem Soc 112:7803–7804
14. Wang HY, Zhu ZH, Meng DQ, Zhang WX, Liu XY (2001) Chin J Chem Phys 14:0285–0291
15. Gagliardi L, Roos BO (2005) Nature 433:848–851

16. Roos BO, Malmqvist P, Gagliardi L (2006) J Am Chem Soc 128: 17000–17006
17. Gt V, Bickelhaupt FM, Baerends EJ, Fonseca Guerra C, Gisbergen SJA, Snijders JG, Ziegler T (2001) J Comput Chem 22: 931–967
18. Lenthe EV, Baerends EJ, Snijders JG (1993) J Chem Phys 99:4597
19. Lenthe EV, Baerends EJ, Snijders JG (1994) J Chem Phys 101:9783
20. Lenthe EV, Baerends EJ, Snijders JG (1999) J Chem Phys 110:8943
21. Perdew JP (1986) Phys Rev B 33:8822–8824
22. Perdew JP (1986) Phys Rev B 34:7406
23. Perdew JP, Wang Y (1992) Phys Rev B 45:13244–13249
24. Becke AD (1986) J Chem Phys 84:4524
25. Becke AD (1993) J Chem Phys 98:5648
26. Shannon RD (1976) Acta Crystallogr Sect A 32:751–767
27. Lyon JT, Hu HS, Andrews L, Li J (2007) Proc Natl Acad Sci USA 104:18919–18924
28. Zhang YG, Li YD (2010) Chin Phys B 19:033302
29. Moskaleva LV, Matveev AV, Rösch N (2006) Chem Eur J 12: 629–634
30. Moskaleva LV, Matveev AV, Dengler J, Rösch N (2006) Phys Chem Chem Phys 8:3767–3773
31. Hoe WM, Cohen AJ, Handy NC (2001) Chem Phys Lett 341: 319–328
32. Zhang Y, Wu AA, Xu X, Yan YJ (2006) Chem Phys Lett 421:383–388
33. Lenthe EV, Baerends EJ (2003) J Comput Chem 24:1142
34. Lenthe EV, Snijders JG, Bearends EJ (1996) J Chem Phys 105:6505
35. Blaise J, Wyart JF (1992) International tables of selected constants, energy levels and atomic spectra of actinides, vol 20. Tables of Constants and Numerical Data, Paris, 1992. Taken from http://www.lac-psud.fr/Database/Contents.html
36. Li P, Jia TT, Gao T, Li G (2012) Chin Phys B 21:043301
37. Lyon JT, Andrews L, Malmqvist P, Roos BO, Yang T, Bursten BE (2007) Inorg Chem 46:4917
38. Kahn SD, Pau CF, Chamberlin AR, Hehre WJ (1987) J Am Chem Soc 109:650–663
39. Gopinathan MS, Valency KJ, Theoret I (1983) Chim Acta (Bed) 63: 497–509
40. Nalewajski RF, Mrozek J (1994) Inter J Quant Chem 51:187
41. Roos BO, Borin AC, Gagliardi L (2007) Angew Chem Int Ed 46:1469
42. Rao LF (2011) Progess Chem 23:1295–1307
43. Ochterski JW (2012) Themochemistry in Gaussian, http://www.gaussian.com (accessed Jun 18, 2012) http://www.gaussian.com/g_whitepap/thermo.htm
44. James AM (1992) Lord MP Macmillan's chemical and physical data. Macmillan, London
45. Enthalpy of atomization: periodicity, taken from http://www.webelements.com/periodicity/enthalpy_atomisation/
46. Huber KP, Herzberg G (1979) Molecular spectra and molecular structure. Constants of diatomic molecules. Van Nostrand Reinhold, New York
47. Green DW (1980) Int J Thermophys 1:61–71
48. Baerends EJ, Branchadell V, Sodupe M (1997) Chem Phys Lett 265: 481–489